Design and Simulation of Micromachined Gyroscope

N. AbuAlarraj, H. Hassan, and H. Ibrahim
Electronics and Communications Engineering
Arab Academy for Science and Technology and Maritime Transport
EGYPT

Abstract: - In this paper a MEMS vibrating rate gyroscope design based on previous work [1] was analyzed to get its mechanical characteristics. In this design, bended beams were used for the inner and outer structures. Electrostatic force is applied on the comb drive electrodes of the gyroscope to create motion in the drive mode direction. The excitation of the gyroscope's drive mode and the deflection of the inner mass due to Coriolis force is simulated using ANSYS FEA software. The simulation results show resonance frequencies of 3769 *Hz* for the drive mode and 3661 *Hz* for the sense mode, maximum displacement of 5.07 *μm* in drive mode and 6.89*nm* in sense mode, the mechanical sensitivity is 0.00689 *μm/ (°/s)*, and the frequency mismatch of 2.86*%*.

Key-Words: - MEMS gyroscope, Mechanical coupling, FEA, Low spring-constant, Electrostatic

1 Introduction

Micromachined inertial sensors are a very versatile group of sensors with applications in many areas. Until recently, medium to high performance inertial sensors were restricted to applications in which the cost of these sensors was not of crucial concern, such as military and aerospace systems. Commercial applications already exist, mainly in the automotive industry for safety systems such as airbag release, seat belt control, active suspension, and traction control. Inertial sensors are used for military applications such as inertial guidance and smart ammunition. Recently various types of MEMS gyroscope fabricated with new microfabrication technologies which use separate oscillation modes for drive and sense, have been developed [2-10]. In these gyroscopes, the sensitivity improves as the frequency mismatch between the two modes decreases. Several prototype gyroscopes have been tested and have shown promising results in a range of ±700 deg/s [5].

In this paper a simulation of MEMS vibrating rate gyroscope design is demonstrated using FEA software (ANSYS) to measure different mechanical characteristics. The structure of the Gyroscope is shown in Figure.1. The material used is silicon and it is driven by means of comb electrodes [6]. The main sources of errors of comb driven gyroscopes are mechanical and electromechanical coupling effects and the small deflections which are to be measured. The inner mass and outer mass are suspended using four beams. The mass oscillates along the *x*-direction (drive mode). An externally induced rotation about the *y*-axis (angular rate Ω) produces a deflection in the *z*-direction due to the Coriolis force (sense mode). This deflection is detected as a change in the capacitance between the mass and the detection electrodes.

2 Gyroscope Design

2.1 Structure

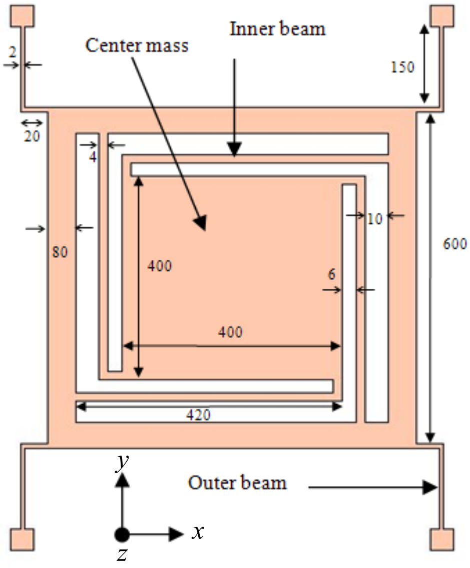

Fig.1 Physical dimensions of the MEMS Gyroscope

The dimensions of the gyroscope investigated are shown in Fig.1. The inner mass is 400μm×400 μm×40 μm in size. The support beams of the inner mass have a width (w) of 4μm and height (h) of 9.25μm. The size of the outer mass is 600μm×600 μm ×40 μm. The outer support beams have each a width (w) equal to 2 μm and height (h) 40 μm. Two electrodes lie beneath the inner mass for detection. The gyroscope is designed in a way such that little deflection occurs in the inner beams when the outer beams are bent due drive mode. In sense mode, the inner beams are deflected while the outer beams experience little bending. Any change in the position of the inner mass changes the capacitance between the mass and detection electrodes [7]. This indicates that the outer and inner beams are rigid with respect to the z- and x-directions, respectively. Thus, the two pair of beams move independently in the two modes. Drive mode oscillations have little effect on the beams used in the detection mode because the coupling between the modes is very weak.

2.2 *Design*

A simple model of the MEMS gyroscope is shown in Fig.2. In drive mode, a force (*$F(t)=F_d$ sinwt*) vibrates the mass along the x-axis. A Coriolis force (*Fc*) is induced in the z-direction when the mass is subjected to a constant angular rate (Ω). The equation of motion that describes this behavior is [1]:

$$m\ddot{x} + c_x\dot{x} + k_x x = F_d \sin\omega t \tag{1}$$

$$m\dot{z} + c_z\dot{z} - 2m\Omega\dot{x} + k_z z = 0 \tag{2}$$

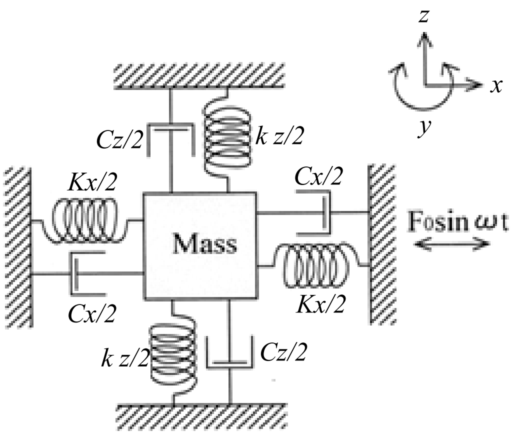

Fig.2 Simple model of vibrating gyroscope [1]

where m is the mass; c_x and c_z are the resistances due to damping, and k_x and k_z are the spring- constants for the x- and z-directions respectively. The spring-constants are calculated by [8]:

$$k_x = \frac{Ehw^3(4L_b \times L_a)}{L_b{}^3(L_a + L_b)} \tag{3}$$

$$k_z = \frac{4Ew\left(\frac{h}{L_a}\right)^3}{1 + \frac{L_b}{L_a}\left(\left(\frac{L_b}{L_a}\right)^2 + 12\frac{1+v}{1+\left(\frac{w}{h}\right)^2}\right)} \tag{4}$$

where E is the Youngs Modulus and h is the height of the structure.

A schematic of the crab-leg suspension is shown in Fig.3. The force resulting from the electrostatic actuation of the comb-drive is equal to [9]:

$$F_d = \frac{\varepsilon_o N\,h\,V_{dc}^{\,2}}{g_o} \tag{5}$$

When the mass is driven such that it oscillates at the resonance frequency, the oscillatory motion derived from Eqs. (1) and (2) is [1]:

$$x(t) = -x_m \cos\omega_x t \tag{6}$$

$$Z(t) = \frac{2m\Omega\omega_x x_m}{k_z}\frac{1}{\sqrt{\{1-(\omega_x/\omega_z)^2\}^2+(\omega_x/\omega_z)^2}} \times \sin\omega_x t - \varphi \tag{7}$$

where x_m is the amplitude at resonance for the x-direction and is equal to:

$$x_m = \frac{F_d Q_x}{k_x} \tag{8}$$

$$\varphi = \tan^{-1}\frac{\lambda}{Q_y(1-\lambda)^2} \tag{9}$$

$$\lambda = \frac{\omega_x}{\omega_z} \tag{10}$$

The resonance quality factor for the x- and z-directions respectively is given by:

$$Q_x = \frac{m\,\omega_x}{c_x}, \qquad Q_z = \frac{m\,\omega_z}{c_z} \tag{11}$$

where ω_x and ω_z are the resonant frequencies.

$$\omega_x = \sqrt{\frac{k_x}{m_x}}, \qquad \omega_z = \sqrt{\frac{k_z}{m_z}} \tag{12}$$

The Coriolis force (F_c) is equal to:

$$F_c = 2m\,\Omega\dot{x} = \frac{2m\,\Omega\,\omega_x\,Q_x\,F_d}{k_x} \tag{13}$$

For matched mode operation, this force results in a sense mode displacement at resonance of:

$$y = \frac{Q_y\,F_c}{k_y} \tag{14}$$

If the drive amplitude is constant, then the amplitude of the resulting oscillatory motion is proportional to the angular rate *(Ω)*. Furthermore, the sensitivity of the gyroscope ($|y/\Omega|$) is higher when the frequency mismatch ($|\Delta\omega|=|\omega_x-\omega_z|$) is small.

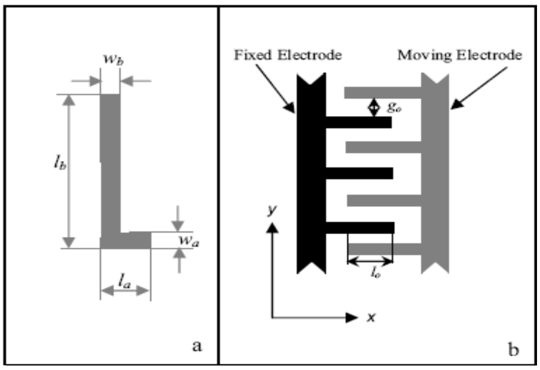

Fig.3 Parts of vibrating gyroscope (a) Crab-leg beam (b) part of the comb-drive

3 Results and Discussion

Simulation of the gyroscope was done in ANSYS FEA. Similar gyroscope wore simulated using ANSYS [10].The structure was meshed as shown in Fig.4 and boundary conditions and constraints were applied on it. The motion of the structure in drive mode and sense mode are shown in Fig.5 and Fig.6 respectively. Fig.7 shows the frequency response of the drive and sense modes. At resonance, the drive mode reaches a maximum displacement of 5.07 *μm* in the x-direction while the sense mode reaches a maximum displacement of 6.89*nm* in the z-direction. These values are computed for an input rotation rate of 1 °/s. The mechanical sensitivity is 0.00689 *μm/(°/s)*. The frequency mismatch between the drive and detection modes is equal to 2.86%. A summary of the gyroscope analytical and simulated results are listed in Table 1. Good agreement between the analytical and the simulated results was established.

Table 1
Parameters and Results of the gyroscope structure

MEMS Gyroscope Parameters		
Quality Factor (*Q*)	100	
Drive Force (F_d)	0.885 *μN*	
Mass (m_x)	34×10^{-9} *kg*	
Mass (m_z)	16.64×10^{-9} *kg*	
Results	**Measured**	**Simulated**
Natural frequency ($\omega_x = 2\pi f_{drive}$) *rad/sec*	2π(3485.23)	2π(3769)
Natural frequency ($\omega_z = 2\pi f_{sense}$) *rad/sec*	2π(3484.95)	2π(3661)
Drive Amplitude (X_m) *μm*	5.44	5.07
Mechanical Sensitivity ($|y_s/\Omega|$) *μm/(°/s)*	0.00791	0.00689

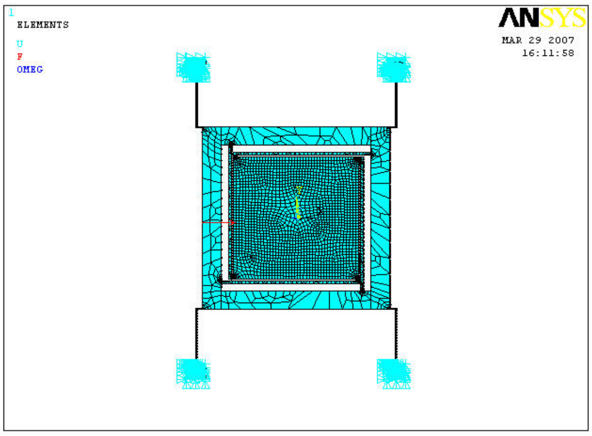

Fig.4 Meshing of the structure in ANSYS

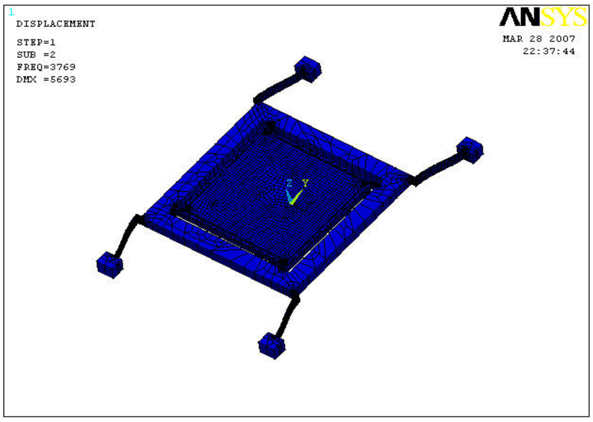

Fig.5 Drive mode in ANSYS

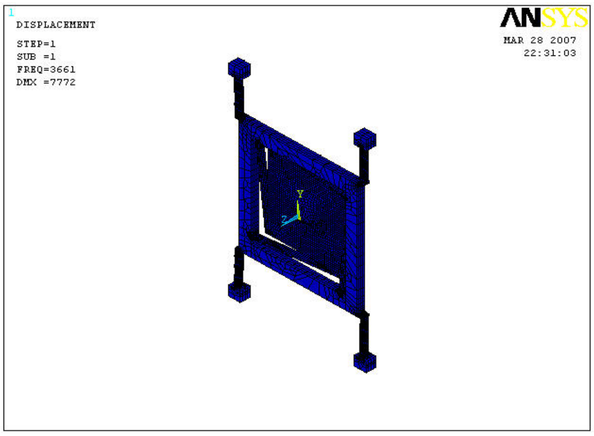

Fig.6 Sense mode in ANSYS

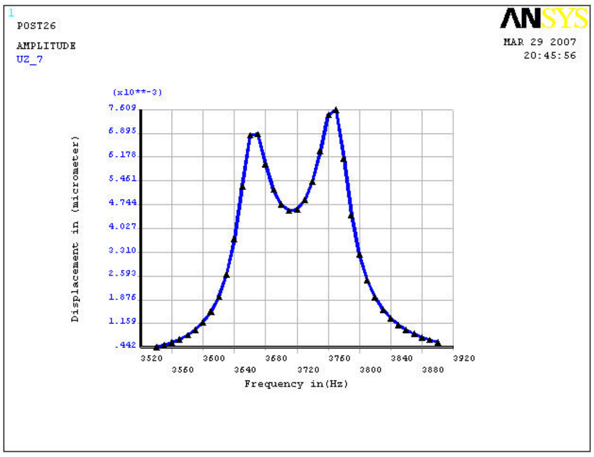

(a)

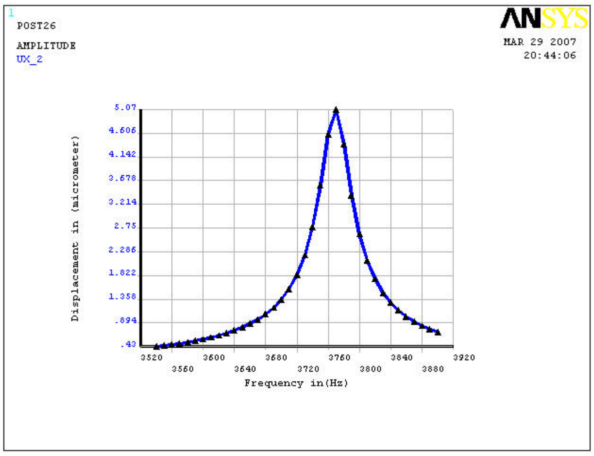

(b)

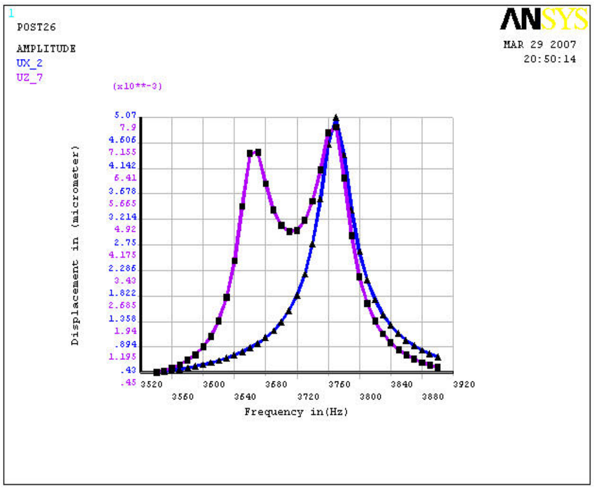

(c)

Fig.7 Displacement vs. Frequency response (*ω_x and ω_z*) for (a) Drive mode (b) Sense mode (c) Drive and Sense modes.

4. Conclusion

A MEMS Gyroscope with independent beams for the drive mode and sense mode was investigated. Good precision between the simulated and the analytical results was obtained. The mechanical resonance frequency and sensitivity were enhanced. Applications that could benefit from this gyroscope include but not limited to space and maritime navigation systems, guided missiles, submarines, etc.

References:

[1] Yoichi Mochida, Masaya Tamura, Kuniki Ohwada, “A micromachined vibrating rate gyroscope with independent beams for the drive and detection modes”, Sensors and Actuators .vol.80, 2000.pp170–178.

[2] Stephen Beeby , Graham Ensell, Michael Kraft, Neil White, “MEMS Mechanical Sensors” A retch House, INC. London, 2004.

[3] Navid Yazdi, F. Ayazi, and Khalil. Najafi, August 1998, Proceedings of IEEE, vol.86, 1640.

[4] Mohamed Gad-el-hak, ,”The MEMS Handbook”, CRC press, LLC. 2002.

[5] F. Paoletti, M.A. Gretillat, N.F. de Rooij, “A silicon micromachined vibrating gyroscope with piezoresistive detection and electromagnetic excitation”, Proc. MEMS ‘vol.96, Atlanta, GA, 1996, pp. 162–167.

[6] K. Maenaka, T. Fujita, Y. Konishi, M. Maeda, “Analysis of a Highly Sensitive Silicon Gyroscope with Cantilever Beam as Vibrating Mass”, Sensors and Actuators A vol.54, 1996.pp568–573.

[7] K. Tanaka, Y. Mochida, S. Sugimoto, K. Moriya, T. Hasegawa, K. Atsuchi, K. Ohwada, “Micromachined vibrating gyroscope”, Proc. MEMS ‘ vol.95, Amsterdam, The Netherlands, 1995. pp. 278–281.

[8] Fedder G K "Simulation of microelectro- mechanical systems" Ph.D. dissertation Dept. Elect. Eng. Comput. Sci., (Univ. California at Berkeley, Berkeley, CA). 1994.

[9] William C. Tang, et. al, 1990, sensors and Actuators A, pp.21-23, vol.328.

[10] Abdelhameed Sharaf, Sherif Sedky, S E -D Habib,’’ Design and Simulation of a New Decoupled Micromachined Gyroscope” Journal of Physics: Conference Series vol.34 pp.464–469(2006)